Light Absorption Enhancement in thin Film GaAs Solar Cells Using Dielectric Nanoparticles

Fateh A. Chaudhry
GDAF-UC3M, Universidad Carlos III de Madrid
Lorena Escandell
GDAF-UC3M, Universidad Carlos III de Madrid
Eduardo López-Fraguas
GDAF-UC3M, Universidad Carlos III de Madrid
Ricardo Vergaz
GDAF-UC3M, Universidad Carlos III de Madrid
Jose Manuel Sanchez-Pena
GDAF-UC3M, Universidad Carlos III de Madrid
Braulio Garcia-Camara (braulio.garcia@uc3m.es)
GDAF-UC3M, Universidad Carlos III de Madrid

Research Article

Keywords: GaAs solar cell, nanostructure, materials, efficiency, short-circuit current

Posted Date: February 15th, 2022

DOI: https://doi.org/10.21203/rs.3.rs-1317819/v1

Abstract

Cost-effective and lightweight solar cells are demanded in strategic fields such as space applications or integrated-wearable devices, among others. A reduction of the thickness of the active layer, producing thin-film devices, has been a traditional solution for both requirements. However, this also reduces the efficiency of the device. For this reason, alternative strategies are being proposed. In this work, light trapping effects of an array of semiconductor nanoparticles located on the top surface of a thin-film GaAs solar cell are investigated to improve the optical absorption and current density in active layer, under the standard AM-1.5 solar spectrum. The numerical results are compared with other previous proposals such as an aluminum nanoparticle array, as well as conventional solar cells with and without a standard anti-reflective coating (ARC). The inclusion of semiconductor nanoparticles (NPs) shown an improved response of the solar cells at different angle of incidence in comparison to solar cell with an ARC. Furthermore, the efficiency was increased a 10% respect to the aluminum nanoparticles (NPs) architecture, and a 21% and a 30% respect to solar cells with and without ARC, respectively.

Introduction

Solar energy is one of the most relevant sustainable energy sources which related technology is in an advanced step. Consequently, it must be part of the solution to current energetic and climatic problems. To satisfy this challenge, solar cell technology should also be able to adequate its characteristics to market requirements. In this sense, present market demands cost-effective and lightweight devices with remarkable power conversion efficiency to provide a massive expansion of their use and also its integration in mobile and wearable devices [1].

Solar devices of the so-called second generation are also known as thin-film devices because they consider reduced dimensions of the active layer. Unfortunately, a reduction of the semiconductor material amount not only involves a decrease of the cost and the weight but also a dramatic decrease of the conversion efficiency. The consequent generation, the third one, came to solve this under different approaches [2–5]. Multi-junction devices with several stacked active layers working at different and complementary spectral ranges, or new materials (e.g., perovskites) are some of the successful alternatives [6, 7]. Additionally, the control over light arose as an interesting strategy to increase the solar cell efficiency by maximizing the amount of light within the active layer. Following this idea, optical elements such as textured electrodes [8], integrated Bragg reflectors [9], diffractive gratings [10, 11], photonic crystals [12], resonant nanostructures [13, 14] or nanoparticles producing up-conversion effects [15] have been included. In this framework, resonant nanoparticles are able to confine light in a sub-wavelength volume and scatter it with a certain directional control. For this reason, their inclusion in solar cells has been analyzed since several years ago [15, 16]. Depending on the aimed dominant effect, these nanoparticles may be placed on the top, inside or at the bottom part of the devices. From a general point of view, their effects can be summed up as the reduction of both reflection and parasitic losses, and the increase of the optical path of the photons inside the active layer. While several works have been mainly focused on the use of plasmonic nanoparticles [17–19], their ohmic losses and low thermochemical

stability [20] may reduce the lifetime of the device. In contrast, recently dielectric resonant nanostructures are also being considered [21–23].

On the other hand, while Silicon has still a dominant position in the photovoltaic industry, other different materials are also in a mature position to fabricate solar cells. This is the case of gallium arsenide (GaAs) which presents efficiencies comparable to silicon in single crystalline devices. Its interesting properties, like its high photoelectric conversion efficiency per mass density, make it suitable for thin-film solar cells [24]. Additionally, other relevant properties such as low temperature coefficient and radiation resistance make it also an excellent material for space and high-altitude platforms [25].

In this work, we demonstrate the successful operation of a thin-film GaAs solar cell including resonant dielectric nanoparticles on the top surface. These nanoparticles were placed with the aim of reducing the surface reflection but also to efficiently scatter light into the solar device. A numerical optimization process, regarding both the material and the geometrical properties of the nanostructures, has been carried out, carefully analyzing the spectral profiles of the total reflectance and absorption rate, as well as the current density. The considered optimal device shows a remarkable rise of the solar cell performance, with a relative increase larger than 20% compared to other devices in the state of the art, like antireflection coatings (ARC) [26, 27] and plasmonic nanoparticles [28–30]. Moreover, the considered geometry has been designed with intention of ease fabrication in contrast to other complex shapes like nanopyramids or nanocones.

Setup And Methods

A unit cell of the proposed device is shown in Figure 1. This is a gallium arsenide (GaAs) solar cell, which arrangement, materials, and geometrical parameters are similar to those considered in previous works [31, 32]. Although this model also includes on the top surface a resonant dielectric nanoparticle to improve the light trapping inside the solar device.

The different component layers are the following ones from top to bottom: cylindrical dielectric nanoparticle (NP) on the top which diameter d, thickness t and material will be optimized, a silicon dioxide (SiO_2) layer of 25 nm acting as space layer, an indium gallium phosphide (InGaP) window layer of 30 nm, a GaAs active layer of 500 nm, a InGaP back-surface-field (BSF) layer of 500 nm, and a GaAs substrate with a large thickness in comparison to the other layers. In order to find an optimal optical operation, the period (w) of the nanoparticles array have been also varied.

It is important to remark that a realistic solar device requires other layers, such as those n- and p-doped layers generating a suitable electric field to separate the photogenerated carriers, as those described in [32]. However, their thickness and low refractive index contrast make them negligible in such an optical analysis as the one we present here. Nevertheless, we previously checked it by using the refractive indexes from reference [33], not having any effect in the results to be presented. For this reason, they are not included in this simplified structure.

We use the finite element method (FEM) implemented by COMSOL Multiphysics © to simulate the optical behavior of the device and the absorption rate of each layer. We set periodic boundary conditions (see unit cell at Figure 1a) to model a periodic array of the unit cell while perfect matched layers are set at the top and bottom absorbing boundaries. The different media are considered isotropic with realistic and complex refractive indices obtained from SOPRA database [34].

The internal (IQE) and external (EQE) quantum efficiencies are common parameters to characterize photovoltaic devices. It is also widely accepted in optical analysis of these devices to consider an IQE of 100%. This means that each absorbed photon creates one electron-hole pair. Consequently, the optical performance of the device through this assumption retrieves a maximum value of the EQE. Another way to characterize the performance of the device is by calculating the short-circuit current density (J_{SC}) in the active layers by the following integration over the spectral range.

$$J_{SC} = \int q\frac{\lambda}{hc} WDA(\lambda) \cdot P_{AM1.5}(\lambda) \cdot d\lambda$$

1

where q is the electron charge, c is the speed of light in vacuum, h is the Planck's constant, and $P_{AM1.5}$ is the standard solar incident irradiance AM1.5G (1000 W/m2). The wavelength-dependent absorbance, WDA(λ) has been calculated through the power loss function. To compute it, the absorbed power density in each layer of the device, and in particular in the active layer, is divided by the input power, and then integrated over the layer volume.

Finally, and for the sake of comparison, we also consider two other systems: a GaAs solar cell with the same geometrical and materials composition as the previous one but without any light-trapping technique, and a similar GaAs solar cell as this latter one but including a typical antireflection coating (ARC) made of magnesium fluoride (MgF_2) and zinc sulfide (ZnS). This allows us to contrast our results with those references, evaluating the achievements of the proposed system in comparison to other well-known configurations [31].

Results And Discussion

As it was previously stated, the aim of this work is to maximize the absorbance on the active layer of a conventional GaAs solar cell by taking advantage of light resonances of dielectric nanoparticles located on top of it. To optimize this arrangement, we previously made a search of the adequate geometrical properties; these are the height, diameter, and array period of the nanoparticles. Additionally, different potential dielectric materials have been also considered. After this recursive analysis and also comparing the results in terms of absorption and reflection with previous works [31], we observed that the geometrical properties providing the best results within the solar spectrum are a diameter (d) of 50 nm, a height (h) of 50 nm and a period w=250 nm. Regarding the material of the nanoparticles, the results are limited to two different dielectric materials: TiO_2 and AlAs. Again, although we tested the results with

several materials, these provided valuable results, for this reason hereinafter only those two dielectric materials are considered. In the last years, there can be found several ways to properly fabricate this kind of ordered arrays in an accurate way, so the geometrical properties are in accordance with the state of the art [35, 36, 37].

Figure 2 shows both the absorbance in the active layer (Figure 2a) and the total reflectance of the device (Figure 2b) as a function of the incident wavelength of a GaAs solar cell with different approaches and under a normal incidence. In particular, these figures show the cases of a conventional GaAs solar cell, a GaAs solar cell with an antireflection coating, a GaAs solar cell including plasmonic (Al) nanoparticles like in [31] and a GaAs solar cell with dielectric nanoparticles on top of it made of either TiO_2 or AlAs as proposed in this work. The resonant behavior of these dielectric nanoparticles produces a strong confinement of light around them that is consequently reemitted to their bottom part, reducing the reflectance and increasing the amount of light going inside the photovoltaic device. The material and size of the nanoparticles as well as its arrangement allows us to select the bandwidth of these effects, matching them with the absorption window of the active material.

As it can be seen, all the considered cases provide an increase of the absorbance from 400 to 850 nm as well as a reduction of the total reflectance, maximizing the amount of light reaching inside the active layer and consequently increasing the amount of photogenerated electron-holes pairs. However, the results of each technique are quite diverse. For instance, the inclusion of an ARC improves the optical absorbance mainly at large wavelengths (600-850 nm), as it can be seen in Figure 2a. It also reduces the total reflectance in this spectral range, but its effects are remarkably worse at the lower end of the solar spectrum (Figure 2b). On the other hand, the inclusion of resonant nanoparticles at the top part of the solar device provides an overall increase of the absorbance and a reduction of the total reflectance compared to the conventional case. Nevertheless, we can still highlight remarkable differences between the metallic and dielectric cases.

Regarding the active absorbance, it can be seen that dielectric nanoparticles (TiO_2 or AlAs) supporting Mie resonances [38, 39] provide a larger boost of the absorbance and in a wider spectral range than plasmonic nanostructures (Al). It is worth mentioning that the case of AlAs nanoparticles provides the best results in terms of absorbance, mainly due to the improvement, with a value up to a 40% higher than the conventional solar cell, in the absorbance in the blue part of the visible spectrum (400-500nm). In addition, the optical properties of these dielectric materials in the solar spectrum present a noticeable lower light absorption than that of metals (due to a lower imaginary part of its refractive index), strongly reducing the thermal effects produced in the case of Al nanoparticles. In the case of the total reflectance (Figure 2b), the effects of both metallic and dielectric nanostructures are similar: a general reduction of the reflectance compared to the conventional solar cell. Even so, again the effects of the dielectric particles are slightly better than those of the metallic ones, in particular in the UV range (< 400 nm) and at large wavelengths (> 600 nm).

While the maximum sensitivity of conventional solar cells is produced under a normal incidence, the addition of a textured or a nanostructured top surface may also increase the performance of the proposed device under non-normal incidence angles. In this sense, Fig. 3 shows a comparison of the spectral evolution of both the absorbance (left panel) and the reflectance (right panel) of a conventional solar cell, a solar cell including an antireflection coating and our proposed device including dielectric nanoparticles on the top surface under different angles of incidence. In particular, we consider an incidence of 20º, 40º and 60º as significant examples.

From an overall view of the results, it can be seen that the approach using AlAs nanoparticles provides the best results at any non-normal incidence in terms of both absorbance in the active layer and total reflectance. In the case of the absorbance (Figs. 3a, 3c and 3e), it can be observed that the use of these NPs in the top layer provides a smoother spectral response than the ARC case, as will be explained, and similar to that of a conventional solar cell. Moreover, this absorbance is larger than that of the conventional one at any wavelength in the range between 400 nm and 850nm. This enhancement is maintained for all the explored angles in the 500-800nm range. The improvement only decays in the 400-550 nm range at high angles. The maximum increase is estimated to be around a 44% compared to the conventional solar cell and a 33% to the case including an ARC at 440nm and under a normal incidence. The maximum enhancement is shifted at larger wavelengths at high angular incidence. In this sense, under an incidence of 60º the maximum increase is estimated to be around 80% (630 nm) compared to the conventional cell and an 82% (600 nm) compared to the case including an ARC. This effect allows a better performance of the solar cell during a larger number of hours in real installations without using solar tracker systems. Indeed, it is directly related with the total reflectance response in those wavelength intervals (Figures 3b, 3d and 3f), which spectral evolution shows that the minimum reflectance in the case of the solar cell with NPs is in the range between 600 and 700 nm. Again, the reflectance is much smaller within the solar spectrum than that of the other considered cases. In particular, this is clearly observed at incident angles of 20º and 40º (Figures 3b and 3d). The case of 60º (Figure 3f) is much complex because of the interferences produced in the multilayer ARC. Additionally, the differences between this minimum and the reflectance at other wavelengths are more prominent as the incident angle increases. It is also important to highlight the reflectance peaks appearing at ultraviolet wavelengths for the NPs case. These peaks become more prominent and wider as the incident angle increases, producing a lower absorbance of this approach in the spectral range (400-500 nm). However, these values are still better than those of a conventional solar cell.

In contrast to this response, the inclusion of ARC is mainly focused on its influence for normal incidence. The extra layers produce remarkable interferential effects, in both the absorbance and the total reflectance, which are more pronounced as the incident angle increases. This produces a response full of peaks -especially in the lower wavelengths- with mean values lower than the case of the solar cell with nanoparticles. Meanwhile, the behavior of the nanostructured solar cell is quite acceptable, keeping its effect on the improvement of absorbance quite well within the solar spectrum.

In order to examine the origin of these effects with detail, Fig. 4 shows the spatial distribution of the electric-field (left) and the magnetic-field (right) intensity inside the different solar devices we are comparing. While Figs. 4a and 4b corresponds to the conventional solar cell, Figs. 4c and 4d consider a GaAs solar cell with an ARC and Figs. 4e and 4f show the results of the GaAs solar cell with AlAs nanoparticles. All the figures are obtained at an incident wavelength of 620 nm (the one for remarkable differences in Fig. 3) and under four different incidence angles, which are labeled on the bottom part of the figure. These figures consider an air layer on the top part and a unit cell of the solar device. To clarify each structure a scheme of each one is included. It is clearly observed how the ARC (Figs. 4c and 4d) produces a larger concentration of light in the device than in the conventional case (Figs. 4a and 4b). This is more relevant in the layers that are above the active one, producing a certain reduction of the reflectance and an increase of the light reaching the active material. In contrast, the use of nanostructures on top of the device (Figs. 4e and 4f) provides a larger light confinement and also a more efficient guiding of light towards the active layer. In fact, it can be clearly observed that both the electric and the magnetic field are enhanced in this material compared to the previous cases. This phenomenon is mainly due to resonant effects of the nanoparticles with the incident field. The resonant nanoparticles efficiently confined the electromagnetic field and scatter it again towards the bottom part (the active region). Moreover, these effects are remarkably insensitive to the incidence angle, providing better results than the other two considered cases. This shows up that this solution is a promising way to improve the optical performance of solar cells.

Finally, Fig. 5 shows the simulated short-circuit current density (J_{SC}) as a function of the incidence angle. As before and with the aim of comparing, this figure includes a conventional GaAs solar cell, the solar cell with an ARC and the solar cell with nanoparticles on top of it considering two cases: plasmonic Al nanoparticles, and the proposed dielectric AlAs nanoparticles. Again, it can be seen that although ARC improves the electric performance of a standard solar cell, the use of nanostructures on the top layer provides a better performance in a large angular range (J_{SC} is larger than 10 mA/cm2 up to 80º instead of 70º in the ARC case). In this case, while metallic Al NPs, previously proposed in the literature [31], slightly improve the J_{SC} of an ARC solution, the proposed AlAs NPs significantly rises the current density in the angular range from 0º to 70º, producing a much better response of the solar cell than the other considered cases, avoiding also the thermal effects of the plasmonic nanoparticles.

Conclusions

The aim of this work is focused on improving the optical response of GaAs solar cells using simple nanostructures (e.g. nanodisks and/or nanocylinders). Following the current state of the art and our previous works, we know that resonant nanoparticles, like plasmonic ones, are able to confine the incident electromagnetic field and then scatter it into the bottom layer. Consequently, the amount of light inside the active layer increases, providing an increase of the absorption and a decrease of the reflectivity of the solar device. However, the properties of these nanostructures, their fabrication and integration in

the solar cell and its potential effect on the electric properties of the device should be carefully analyzed for every case in order to optimize the global performance of the solar cell.

With this in mind, we have numerically analyzed the case of a GaAs-based solar cell, whose use on space missions is remarkable. The proposed nanostructure is one of the most feasible arrangements from an experimental point of view, being composed of nanocylinders or nanodisks, depending on the aspect ratio. Additionally, the nanostructure is placed on the top of the device, simplifying its integration on it and reducing its influence on the electric properties of the solar cell. Furthermore, we have contrasted the numerical results with typical designs in the state-of-the-art, such as a conventional GaAs solar cell, a solar cell with an antireflection coating (ARC) and the solar device including plasmonic nanoparticles.

Our optical simulations showed that the use of AlAs nanoparticles is the best and simplest approach to efficiently confine the light, reducing the reflectance and increasing the absorbance of the solar device. This improvement is observed all over the solar spectrum, under a wide angular incidence and compared to the other considered cases. In fact, the spatial distribution of the electromagnetic field shows that these nanoparticles are able to guide the incident light into the active layer in a more effective way than an ARC. In particular, it has been estimated that the short-circuit current density (J_{SC}) using AlAs nanoparticles is 19.34 mA/cm^2 at normal incidence. This is a relative increase of a 30% and a 21% when compared to a conventional GaAs solar cell and a GaAs solar cell with an ARC, respectively. Also, the dielectric nature of these nanoparticles avoids the thermal effects of the plasmonic nanoparticles (e.g. Al) which might involve harmful effects on the electric performance and/or the lifetime of the device.

In summary, this study reveals how the use of semiconductor nanoparticles can improve the optical performance of GaAs-based solar cells with no further antireflective coatings inclusion, improving the optical absorbance and reducing the reflectivity by means of light trapping effects, as well as avoiding unwanted thermal effects.

Declarations

Data Availability

The datasets generated and/or analysed during the current study are not publicly available because they have been generated using COMSOL Multiphysics but are available from the corresponding author on reasonable request.

Acknowledgements

This work was funded by the Spanish Research Agency (AEI), PID2019-109072RB-C31/AEI/10.13039/501100011033, Comunidad de Madrid by SINFOTON2-CM (grant number

S2018/NMT-4326) and by grant PEJD-2018-PRE/IND-9348. These grants are also co-founded by the European Fund for Regional Development.

References

1. S. A. Hashemi, S. Ramakrishna, A.G. Aberle. Recent progress in flexible–wearable solar cells for self-powered electronic devices. Energy Environ. Sci., 13, 685-743 (2020).
2. J. Liu, M. Yao, L. Shen. Third generation photovoltaic cells based on photonic crystals. J. Mater. Chem. C, 7, 3121-3145 (2019).
3. C. Wu, K. Wang, M. Batmunkh, A.S.R. Bati, D. Yang, Y. Jiang,Y. Hou, J.G. Shapter, S. Priya. Multifunctional nanostructured materials for next generation photovoltaics. Nano Energy 70, 104480 (2020).
4. B.M. Rajbongshi, A.Verma (2019) Emerging Nanotechnology for Third Generation Photovoltaic Cells. In: Siddiquee S., Melvin G., Rahman M. (eds) Nanotechnology: Applications in Energy, Drug and Food. Springer, Cham.
5. E.H. Jung, N.J. Jeon, E.Y. Park, C.S. Moon, T.J. Shin, T.-Y. Yang, J.H. Noh, J. Seo. Efficient, stable and scalable perovskite solar cells using poly (3-hexylthiophene). Nature, 567, 511-515 (2019).
6. S. Nordmann, B. Berghoff, A. Hessela, B. Zielinsk, J. John, S. Starschich, J. Knoch. Record-high solar-to-hydrogen conversion efficiency based on a monolithic all-silicon triple-junction IBC solar cell. Sol. Energy Mater. Sol. Cells 191, 422-426 (2019).
7. F. Sahli, J. Werner, B.A. Kamino, et al. Fully textured monolithic perovskite/silicon tandem solar cells with 25.2% power conversion efficiency. Nat. Mater. 17, 820–826 (2018).
8. Y. Özen. The enhancement in cell performance of CdTe-based solar cell with Si/SiO2 distributed Bragg reflectors. Appl. Phys. A. 126, 632 (2020).
9. H.-L. Chen, A.Cattoni, R. De Lépinau, A.W. Walker, O. Höhn, D. Lackner, G. Siefer, M. Faustini, N. Vandamme, J. Goffard, B. Behaghel, C. Dupuis, N. Bardou, F, Dimroth, S. Collin. A 19.9%-efficient ultrathin solar cell based on a 205-nm-thick GaAs absorber and a silver nanostructured back mirror. Nat. Energy, 4, 761-767 (2019).
10. A. Fattah, M. Bavir, A. Abbasi, A.A. Orouji. Efficiency improvement of graphene/silicon Schottky junction solar cell using diffraction gratings. Opt. Quantum Electron. 52, 420 (2020).
11. M.-L. Hsieh, A. Kaiser, S.Bhattacharya, S. John, S.-Y Lin. Experimental demonstration of broadband solar absorption beyond the lambertian limit in certain thin silicon photonic crystals. Sci. Rep. 10, 11857 (2020).
12. Grandidier, D.M. Callahan, J.N. Munday, H.A. Atwater. Gallium Arsenide Solar Cell Absorption Enhancement Using Whispering Gallery Modes of Dielectric Nanospheres. IEEE J. Photovolt. 2, 123-128 (2012).
13. M.H. Elshorbagy, E. López-Fraguas, J.M. Sánchez-Pena, B. García-Cámara, R. Vergaz. Boosting ultrathin aSi-H solar cells absorption through a nanoparticle cross-packed metasurface. Sci. Rep.

202, 10-16 (2020).

14. K.R. Catchpole, A.Polman. Plasmonic solar cells. Opt. Express, 16, 21793-21800 (2008).
15. S. Fischer, A. Ivaturri, P. Jakob, K.W. Krämer, R. Martín-Rodriguez, A. Meijerink, B. Richards, J.C. Goldschmidt. Upconversion solar cell measurements under real sunlight. Opt. Mat., 84, 389-396 (2018).
16. P Spinelli, V.E. Ferry, J. van de Groep, M. van Lare, M.A. Verschuuren, R.E. I. Schropp, H. A. Atwater, A. Polman. Plasmonic light trapping in thin-film Si solar cells. J. Opt. 14, 024002 (2012).
17. H. Atwater, A. Polman, Plasmonics for improved photovoltaic devices. Nat. Mater. 9, 205-213 (2019).
18. W.J. Dong, H. K. Yu, J.-L. Lee. Abnormal dewetting of Ag layer on three-dimensional ITO branches to form spatial plasmonic nanoparticles for organic solar cells. Sci. Rep., 10, 12819 (2020).
19. A. Tooghi, D. Fathi, M. Eskandari. High-performance perovskite solar cell using photonic–plasmonic nanostructure. Sci. Rep., 10, 11248 (2020).
20. V. Thakore, J.Tang, K. Conley, T. Ala-Nissila, M. Karttunen. Thermoplasmonic response of semiconductor nanoparticles: A Comparison with metals. Adv. Theory Simul. 2, 1800100 (2019).
21. S. Das, M.J. Hossain, S.-F. Leung, A. Lenox, Y. Jung, K. Davis, Jr-H. He, T. Roy. A leaf-inspired photon management scheme using optically tuned bilayer nanoparticles for ultra-thin and highly efficient photovoltaic devices. Nano Energy, 58, 47-56 (2019).
22. P.D. Terekhov, K. V. Baryshnikova, Y. Greenberg, Y. H. Fu, A. B. Evlyukhin, A. S. Shalin & A.Karabchevsky. Enhanced absorption in all-dielectric metasurfaces due to magnetic dipole excitation. Sci. Rep. 9, 3438 (2019).
23. M.H. Elshorbagy, E. López-Fraguas, F. A. Chaudhry, J. M. Sánchez-Pena, R. Vergaz, B. García-Cámara. A monolithic nanostructured-perovskite/silicon tandem solar cell: feasibility of light management through geometry and materials selection. Sci. Rep., 10, 1-8 (2020).
24. A. Polman, M Knight; E.C. Garnett, B. Ehrler, W.C. Sinke. Photovoltaic materials: Present efficiencies and future challenges. Science, 352 aad4424 (2016).
25. N. Papež, A. Gajdoš, R. Dallaev, D. Sobola, P. Sedlák, R. Motúz, A. Nebojsa, L. Grmela. Performance analysis of GaAs based solar cells under gamma irradiation. Appl. Surf. Sci. 510, 145329 (2020).
26. M.H. Elshorbagy, K. Abdel-Hady, H. Kamal, J. Alda. Broadband anti-reflection coating using dielectric Si3N4 nanostructures. Application to amorphous-Si-H solar cells. Opt. Commun. 390, 130-136 (2017).
27. Y. Zhang, J. Zheng, C. Fang, Z. Li, X. Zhao, Y. Li, X. Ruan,Y. Dai. Enhancement of silicon-wafer solar cell efficiency with low-cost wrinkle antireflection coating of polydimethylsiloxane. Sol. Energy Mater. Sol. Cells, 181, 15-20 (2018).
28. K. Nakayama, K. Tanabe, H. Atwater. Plasmonic nanoparticle enhanced light absorption in GaAs solar cells, Appl. Phys. Lett. 93, 121904 (2008).
29. G. Singh, S.S. Verma. Plasmon enhanced light trapping in thin film GaAs solar cells by Al nanoparticle array. Phys. Lett. A, 383, 1526-1530 (2019).

30. A.D. Khan, A.D. Khan, F.E. Subhan, M. Noman. Efficient Light Management in Ultrathin Crystalline GaAs Solar Cell Based on Plasmonic Square Nanoring Arrays. Plasmonics, 14, 1963-1970 (2019)
31. L. Yang, S. Pillai & M. A. Green. Can plasmonic Al nanoparticles improve absorption in triple junction solar cells? Sci. Rep. 5,11852 (2015).
32. N.P. Hylton, X.F. Li, V. Giannini, K.-H. Lee, N.J. Ekins-Daukes, J. Loo, D. Vercruysse, P. Van Dorpe, H. Sodabanlu, M. Sugiyama, S.A. Maier. Loss mitigation in plasmonic solar cells: aluminium nanoparticles for broadband photocurrent enhancements in GaAs photodiodes. Sci. Rep. 3, 2874 (2013).
33. E.Ochoa-Martínez, I. Barrutia, M. Ochoa, E. Barrigón, I. García, I. Rey-Stolle, C. Algora, P.Basa, G. Kronome, M. Gabás. Refractive indexes and extinction coefficients of n- and p-type doped GaInP, AlInP and AlGaInP for multijunction solar cells. Solar Ener. Mater. Solar Cell 174, 388-396 (2018).
34. Optical Data from Sopra Database. http://www.sspectra.com/sopra.html (2008)
35. Z. Zhong, B. Gates and Y. Xia. Soft Lithographic Approach to the Fabrication of Highly Ordered 2D Arrays of Magnetic Nanoparticles on the Surfaces of Silicon Substrates. Langmuir 16, 10369-10375 (2000).
36. A.M. Whiticar, E. K. Martesson, J. Nygard, K.A. Dick and J. Bolisson. Annealing of Au, Ag and Au–Ag alloy nanoparticle arrays on GaAs (100) and (111) B. Nanotechnoloy 28, 205702 (2017).
37. Y. Ke, X. Wen, D. Zhao, R. Che, Q. Xiong, and Y. Long. Controllable Fabrication of Two-Dimensional Patterned VO2 Nanoparticle, Nanodome, and Nanonet Arrays with Tunable Temperature-Dependent Localized Surface Plasmon Resonance. ACS Nano 11, 7542-7551 (2017)
38. R. Gómez-Medina, B. García-Cámara, I. Súarez-Lacalle, F. González, F. Moreno, M. Nieto-Vesperinas, J.J. Sáenz. Electric and Magnetic Dipolar Response of Germanium Nanospheres: Interference Effects, Scattering Anisotropy, and Optical Forces. J. Nanophoton. 5, 053512 (2011).
39. J.M. Geffrin, B. García-Cámara, R. Gómez-Medina, et al. Magnetic and Electric Coherence in Forward- and Back-Scattered Electromagnetic Waves by a Single Dielectric Subwavelength Sphere. Nature Commun. 3, 1171 (2012).

Figures

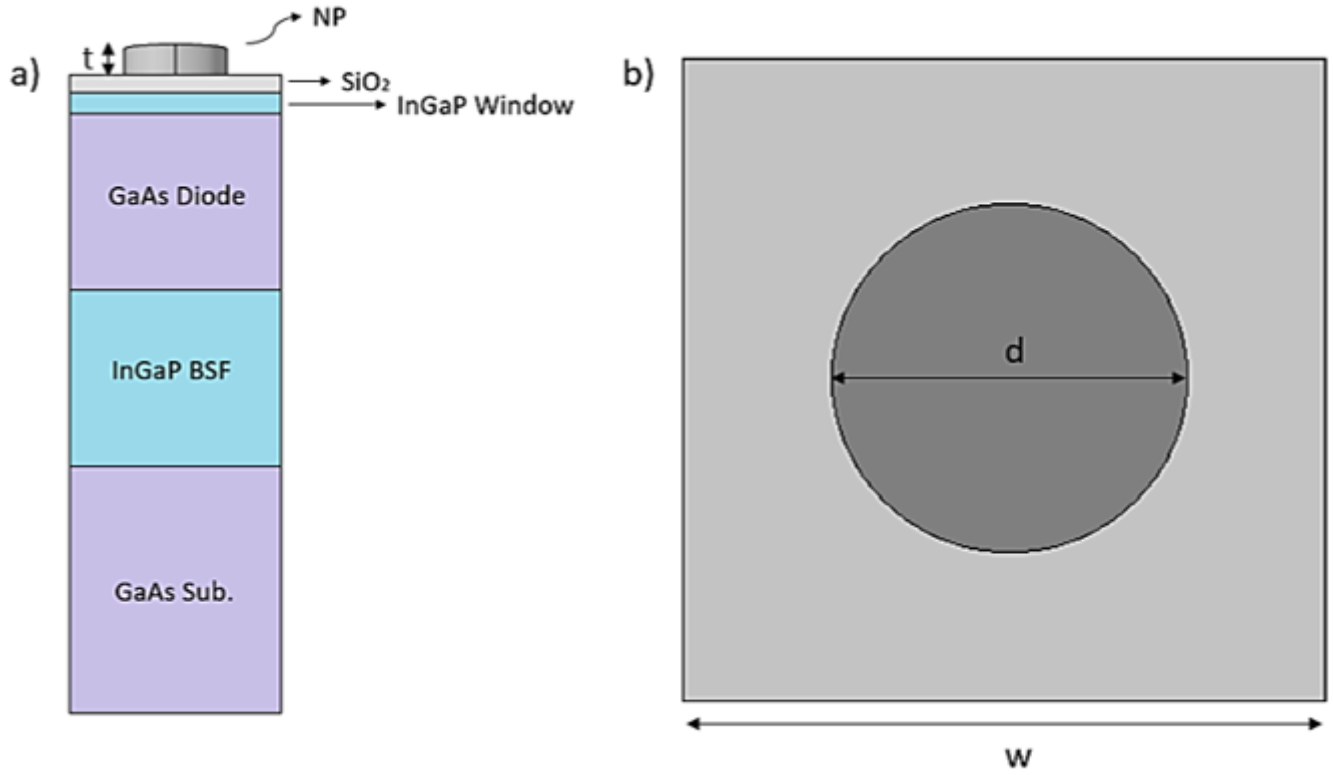

Figure 1

(**a**) Scheme of the proposed GaAs solar cell with dielectric nanoparticles on the front surface. (**b**) Top view of the device, including labels of the main considered geometrical parameters.

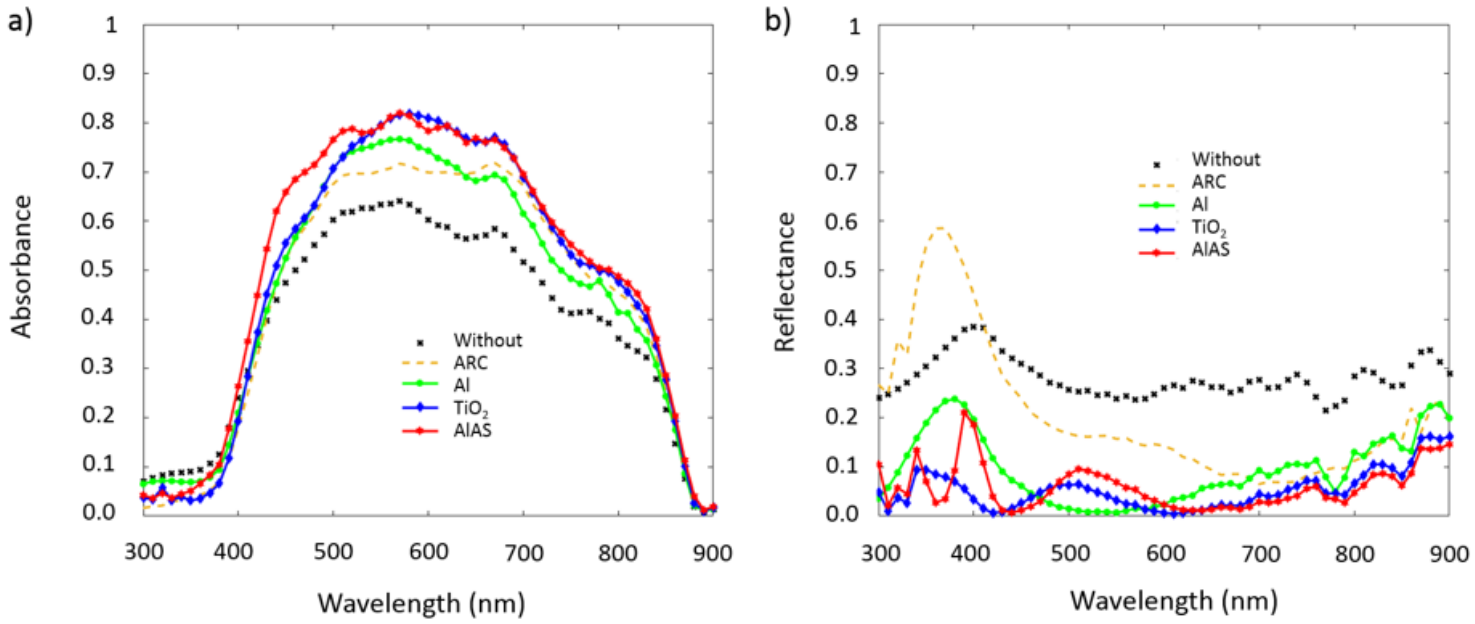

Figure 2

Spectral evolution of **(a)** the absorbance in the active layer and **(b)** the total reflectance of a GaAs solar cell for five different configurations: a conventional device without photonic strategies, a solar cell

including an antireflection coating, a device with aluminum plasmonic nanoparticle on top of it and a solar cell including dielectric nanoparticle on it (TiO_2 or AlAs).

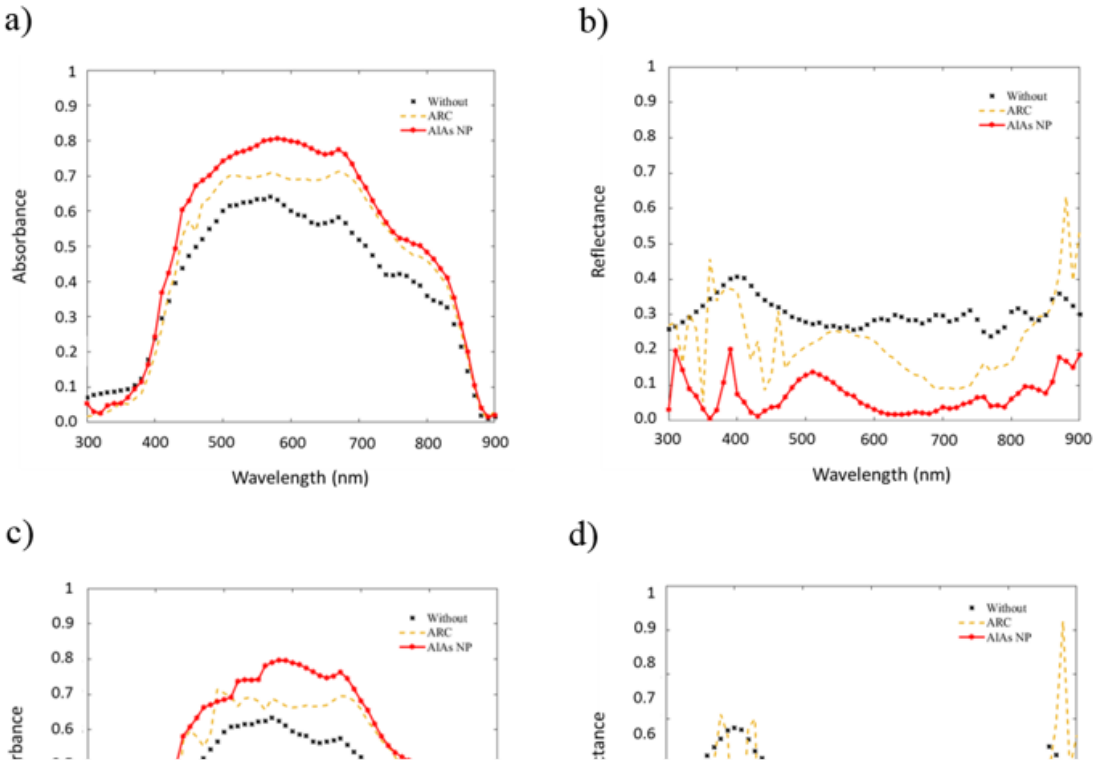

Figure 3

Absorbance in active layer (left) and total reflectance (right) of the device under an incidence of 20° in (a) & (b), of 40° in (c) & (d) and of 60° in (e) and (f).

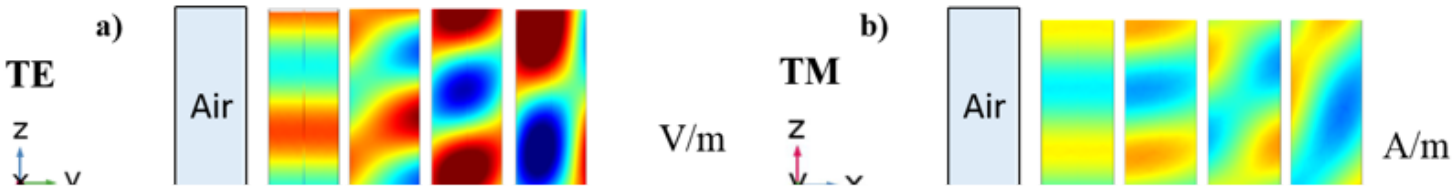

Figure 4

Spatial distribution of the electric and magnetic field intensities in the solar cell. (**a**) Electric field and (**b**) magnetic field distribution in a conventional solar cell. (**c**) Electric field and (**d**) magnetic field distribution in a GaAs solar cell including an ARC. (**e**) Electric field and (**f**) magnetic field distribution in a GaAs solar cell including AlAs nanoparticles on it. All the cases consider four different angular incidences, from left to right: normal (0°), 20°, 40° and 60°.

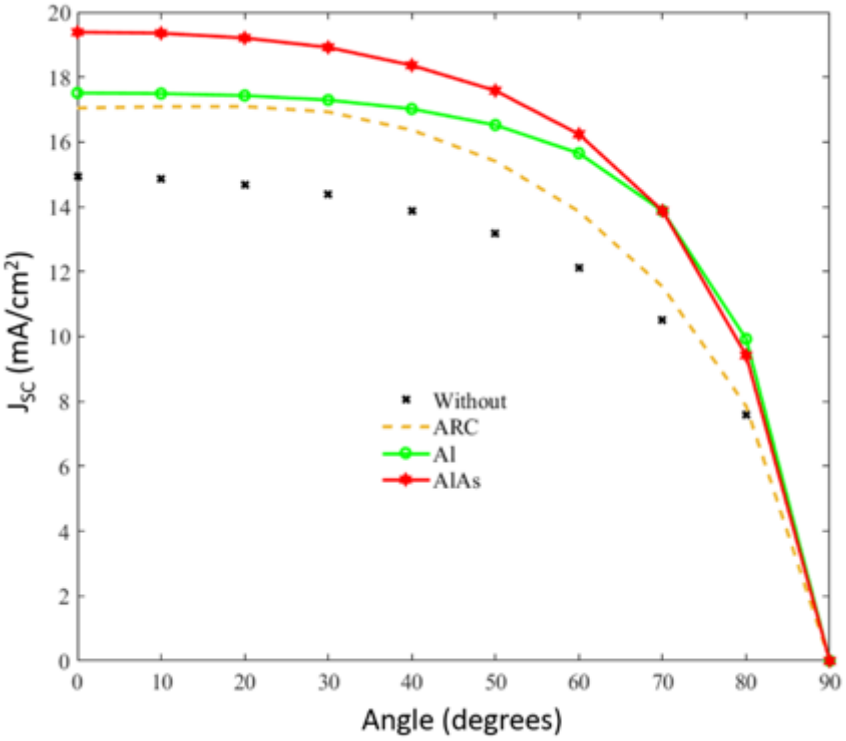

Figure 5

Short-circuit current density (J_{SC}) as a function of the incident angle for the considered cases of a standard GaAs solar cell (x - none line), a GaAs with an ARC (dashed line) and a GaAs with nanoparticles on it. These nanoparticles are either metallic ones (o - solid line) like in ref [Yang 2015] or the proposed dielectric AlAs nanoparticles (hexagram - solid line).